HHS Public Access

Author manuscript

Mucosal Immunol. Author manuscript; available in PMC 2016 July 01.

Published in final edited form as:

Mucosal Immunol. 2016 July ; 9(4): 1015–1026. doi:10.1038/mi.2015.115.

Transforming growth factor-β1 sustains the survival of Foxp3+ regulatory cells during late phase of oropharyngeal candidiasis infection

N Bhaskaran[1], **C Quigley**[1], **A Weinberg**[1], **A Huang**[2], **D Popkin**[3], and **P Pandiyan**[1]

[1]Department of Biological Sciences, School of Dental Medicine, Case Western Reserve University, Cleveland, Ohio, USA

[2]Department of Pathology, School of Medicine, Case Western Reserve University, Cleveland, Ohio, USA

[3]Department of Dermatology, School of Medicine, Case Western Reserve University, Cleveland, Ohio, USA

Abstract

As $CD4^+CD25^+Foxp3^+$ regulatory T cells (T_{regs}) play crucial immunomodulatory roles during infections, one key question is how these cells are controlled during antimicrobial immune responses. Mechanisms controlling their homeostasis are central to ensure efficient protection against pathogens, as well as to control infection-associated immunopathology. Here we studied how their viability is regulated in the context of mouse oropharyngeal candidiasis (OPC) infection, and found that these cells show increased protection from apoptosis during late phase of infection and reinfection. T_{regs} underwent reduced cell death because they are refractory to Tcell receptor restimulation-induced cell death (RICD). We confirmed their resistance to RICD, using mouse and human T_{regs} *in vitro*, and by inducing α-CD3 antibody-mediated apoptosis *in vivo*. The enhanced viability is dependent on increased transforming growth factor-β1 (TGF-β1) signaling that results in upregulation of cFLIP (cellular FLICE (FADD-like IL-1β-converting enzyme)-inhibitory protein) in T_{regs}. Protection from cell death is abrogated in the absence of TGF-β1 signaling in T_{regs} during OPC infection. Taken together, our data unravel the previously unrecognized role of TGF-β1 in promoting T_{reg} viability, coinciding with the pronounced immunomodulatory role of these cells during later phase of OPC infection, and possibly other mucosal infections.

Correspondence: P Pandiyan (pxp226@case.edu).

SUPPLEMENTARY MATERIAL is linked to the online version of the paper at http://www.nature.com/mi

AUTHOR CONTRIBUTIONS

P.P. designed the study, performed experiments, analyzed data, and wrote the manuscript, N.B and C.Q. performed some *in vivo* experiments, D.P. helped with LCMV infection, A.H. contributed to discussions, and A.W. edited the manuscript.

DISCLOSURE

The authors declared no conflict of interest.

INTRODUCTION

$CD4^+CD25^+Foxp3^+$ regulatory T cells (T_{regs}) are central for dominant tolerance to self-antigens and innocuous commensals.[1–3] A majority of T_{regs} are natural or thymic T_{regs}, but a few also arise *in vivo* in the periphery from conventional naive CD4 T cells or can be generated *in vitro*. Reduced frequency of circulating T_{regs} and their defective functions are associated with autoimmunity and inflammation.[4] In contrast, in patients with cancer, T_{reg} enrichment at the tumor sites is implicated in regulating tumor immune-surveillance.[5] As the size of the T_{reg} population determines disease outcomes, manipulating it is an exciting strategy in human immune therapy. Therefore, basic mechanisms of T_{reg} viability and proliferation in different niches are being explored.[6,7] With respect to lymphocyte apoptosis, restimulation-induced cell death (RICD)[8,9] and cytokine withdrawal-induced death[10] govern effector cell homeostasis *in vivo*.[11] RICD, also referred to as activation-induced cell death,[12,13] is responsible for the attrition and homeostasis of expanded T-cell population after antigen clearance.[9,14] RICD is an extrinsic apoptosis mechanism that is signaled through Fas and tumor necrosis factor-α receptors, leading to activation of caspases.[15] Cytokine withdrawal-induced death is an intrinsic mitochondrial apoptosis that occurs because of cellular stressors such as withdrawal of survival cytokines,[16] involving the activation of Bim and caspases.[10,17,18] Interleukin-2 (IL-2) and other γ-chain cytokines control T_{reg} survival, without which T_{regs} are susceptible to Bim-dependent cytokine withdrawal-induced death.[19,20] It is well known that along with T_{regs}, RICD[8,9,21] and cytokine withdrawal-induced death are also[10,16] required for immune homeostasis following antigen clearance during infections.[22,23] Although Bim and transforming growth factor-β1 (TGF-β1) have been implicated in regulating the size of T_{regs},[24,25] their role in T_{reg} RICD is unknown. Two *in vitro* studies have examined RICD in T_{regs}, but the mechanistic details and the physiological relevance were not explored.[26,27] Although $Foxp3^+$ T_{regs} are shown to accumulate at infection sites, little is known about their apoptosis mechanisms and homeostasis during infections.

In the context of microbial infections, T_{regs} perform important roles to limit inflammation, especially at late time points of infection. We and others have previously reported their immune-protective functions that vary depending on the context of infections.[28–31] Here we have systematically shown that T_{regs} resist RICD compared with T effector cells during oropharyngeal candidiasis (OPC) infection and chronic lymphocytic choriomeningitis virus (LCMV) infection. Increased survival is dependent on TGF-β1 signaling and upregulation of cFLIP (cellular FLICE (FADD-like IL-1β-converting enzyme)-inhibitory protein) in T_{regs}. This novel mechanism that offers a survival advantage to these critical immunomodulatory T cells may be important for immune homeostasis and resolution of immunopathology after infection clearance, and possibly other inflammatory conditions.

RESULTS

T_{regs} undergo reduced apoptosis during later phases of oral *Candida* infection and reinfection *in vivo*

As we have previously shown that T_{regs} play important roles in oral candidiasis model,[30] we first sought examine the T_{reg} frequency during the course of OPC infection. We infected

Foxp3^{GFP} reporter mice with *Candida*, isolated the cells from draining cervical lymph nodes (CLNs), and estimated the frequency of Foxp3^{GFP+} cells using flow cytometric analyses. As expected, sham-infected mice showed ~10% of Foxp3^{GFP+} cells among CD4$^+$ T cells (Figure 1a,b). Although on days 1 and 2 there was a drop in the frequency of GFP$^+$ T_{regs}, the frequency of T_{regs} kept increasing even 5 days after infection in the CLNs (Figure 1a,b). We have previously shown that mice clear the infection in ~3–4 days, and in the absence of T_{regs} they succumb to severe infection and immunopathology.[30,31] Although tumor necrosis factor-α has protective functions during acute infection,[32] T_{regs} reduce tumor necrosis factor-α levels in CD4 T cells, thereby limiting tongue inflammation at later time points. Therefore, we hypothesized that T_{regs} may proliferate or survive better over effector cells at later time points, coinciding with immunopathology control. Although Foxp3 + T_{regs} did not proliferate better than Foxp3^{GFP-} T effector cells, they showed increased viability, as measured by propidium iodide (PI) staining (Supplementary Figure S1A online). Fas- and Bim-dependent apoptosis of effector cells,[23,33] along with immunomodulation by T_{regs}, are known to contribute to immune response shutdown and control of immunopathology after infections.[14,28] Because T_{regs} are already known to be susceptible to Bim-dependent apoptosis induced by cytokine withdrawal,[7,19] we hypothesized that their increased viability is attributed to their reduced ability to undergo RICD during infection. Therefore, we induced RICD of T cells *in vivo* by reinfecting Foxp3^{GFP} mice at late time points of primary *Candida* infection. We assessed the viability of the cells on day 1 after reinfection. We harvested the cells from axillary lymph nodes and CLN, the draining lymph nodes, as well as spleen and inguinal lymph nodes to assess CD4$^+$ cell viability. We refer to the non-T_{reg} (Foxp3−) cells activated by the infection *in vivo* as effector cells (T_{effs}). We gated on the control CD4$^+$Foxp3^{GFP-} T_{effs} and CD4$^+$ CD25$^+$Foxp3^{GFP+} T_{regs} (Supplementary Figure S1B, C), and measured the viability by PI staining. We found that the frequency of PI$^+$ dead cells among CD4+Foxp3^{GFP+} T_{regs} was 10–12%, and was significantly lower than in CD4+ Foxp3^{GFP-} effector cells (~24%) in draining lymph nodes (Figure 1c and Supplementary Figure S1C). In addition, by examining the absolute cell numbers *ex vivo* at various time points after primary infection, we found that although the effector cells undergo an expansion followed by contraction at late time points, T_{regs} did not show reduction in cell counts (Supplementary Figure S1D) coinciding to increased survival at later time points. In spleen and inguinal lymph nodes, although T_{regs} had slightly increased viability than effector cells, the differences were smaller than in draining lymph nodes (Figure 1c). Next, we adoptively transferred fluorescence-activated cell sorting (FACS)-sorted naive CD4+CD25−GFP− cells (conventional or control CD4+ cells; T_{cons}) or CD4+CD25+GFP+ T_{regs} into *Rag1*$^{-/-}$ mice, 4 days before primary OPC infection, and assessed their viability 1 day after reinfection. We refer to the non-T_{reg} (Foxp3− T_{cons}) cells activated by the infection *in vivo* as T_{effs}. We found that the frequency of PI$^+$ cells was greater among T_{effs} than T_{regs} (Figure 1d), showing that T_{regs} survive better than conventional CD4 T cells during RICD at late phase of infection. To confirm the role of Fas in the contraction of CD4$^+$ T cells, we infected Fas mutant lymphoproliferation (*lpr*) mice, comparing with the wild-type (WT) mice. Although there was an increase in the frequency of T_{regs} in WT mice, there was no increase in *lpr* mice at late time points (Supplementary Figure S2). These results demonstrate that Fas is largely contributing to contraction of effector cells, without which the apparent increase in proportion of T_{regs} is not observed at late time points.

To further validate that T_{regs} have decreased susceptibility to T cell receptor (TCR)-mediated RICD *in vivo*, we directly examined whether T_{regs} resist α-CD3 antibody-mediated deletion *in vivo*. We injected 100 μg of α-CD3 antibody in $Foxp3^{YFP}$ mice and measured the viability of T_{regs} and conventional $CD4^+$ cells.[34] Correlating to the results from OPC infection experiments, we found that the percentage of PI^+ cells was significantly lower among $Foxp3^{YFP+}$ T_{regs} compared with $Foxp3^{YFP-}$ cells *in vivo* in CLN (Figure 1e), spleen, and other lymph nodes upon α-CD3 antibody injection (Figure 1e,f). To confirm whether T_{regs} resist apoptosis during a chronic infection, we infected the mice with LCMV clone 13, and assessed apoptosis of $CD4^+$ T cells at different time points after infection. We found that at all time points, T_{regs} showed significantly reduced apoptosis than effector cells after infection *in vivo* (Supplementary Figure S3).

Mouse and human T_{regs} are resistant to RICD and show concomitant reduction in active caspase-3 levels

To investigate the mechanism by which T_{regs} resist RICD, we examined their viability during RICD apoptosis *in vitro*. We isolated $CD4^+$ $CD25^+$ $Foxp3^{GFP+}$ cells (T_{reg}) and conventional or control $CD4^+$ $CD25^-$ $Foxp3^{GFP-}$ naive T cells (T_{con}) from $Foxp3^{GFP}$ reporter mice (Supplementary Figure S4) and stimulated and restimulated them with α-CD3 antibody (1 μg ml^{-1}) and IL-2. We measured the cell viability by their forward scatter shift and PI staining 12–18 h after RICD induction using flow cytometry. Whereas 80–85% of the T_{cons} were PI^+, only 30–40% of T_{regs} showed PI staining (Figure 2a). Then, we induced RICD with different concentrations of α-CD3 antibody. We measured apoptosis by annexin-V and PI staining (Figure 2b) and found that T_{regs} underwent significantly reduced apoptosis. Next, we isolated $CD4^+CD25^+$ $CD127^{lo}$ T_{regs} and $CD4^+$ $CD25^-$ T_{cons} from human peripheral blood mononuclear cells and induced RICD. Human T_{regs} also showed resistance to RICD compared with T_{cons} (Figure 2c,d). Upon induction of RICD, both mouse and human T_{regs} showed substantially lower levels of cleaved caspase-3 compared with T_{cons} (Figure 2e,f). Taken together, these results reveal that although conventional CD4 cells are highly susceptible to RICD, T_{regs} show reduced RICD with concomitantly lower levels of active caspase-3.

RICD resistance is not because of retarded proliferation in T_{regs}

Previous studies show that T cells producing high levels of IL-2 and proliferating at higher rates have an increased propensity to die of RICD.[35] T_{regs} produce little or no IL-2 and proliferate slower that might contribute to their reduced apoptosis. IL-2 was ruled out because we added excess of IL-2 during RICD. However, during the initial stimulation for 4 days, T_{regs} displayed reduced proliferation compared with T_{cons} as determined by CPD670 labeling (Figure 3a). We assessed cell death, gating on proliferating and nonproliferating cells, upon RICD. Nonproliferating cells (in the prior stimulation) in both the populations showed little or no apoptosis (Figure 3b,d). However, proliferating T_{regs} were still exquisitely resistant to RICD compared with proliferating T_{cons} (Figure 3c,d). Moreover, 16 h after RICD induction, the time point at which we measured apoptosis, there was no difference in proliferation between T_{cons} and T_{regs} (data not shown). Moreover, to examine whether T_{regs} and T_{cons} are activated at different levels, we tested their nuclear factor (NF)-κB activation by its nuclear translocation. Confocal microscopy revealed that nuclear

translocation of the p65 subunit of NF-κB was comparable in T_{regs} and T_{cons} after RICD stimulation (Figure 3e). These results showed that RICD resistance of T_{regs} is not due to their reduced proliferation or activation.

T_{regs} and *in vitro* T_{regs} resist TCR-mediated RICD and direct Fas-mediated apoptosis

Next, we explored whether TCR-induced RICD was Fas–Fas ligand (FasL) dependent, and therefore induced RICD in the presence or absence of α-FasL antibody. α-FasL antibody abrogated TCR-mediated RICD (Figure 4a), indicating the RICD we observed was Fas–FasL apoptosis. We then analyzed the expression of Fas and FasL at 0 and 6 h after RICD induction. *In vitro* induced T_{regs} are referred to as *in vitro* T_{regs} in our experiments. Although Fas levels were comparable (Figure 4b), T_{regs} and *in vitro* T_{regs} showed reduced FasL expression compared with T_{cons} (Figure 4c). Next, we determined whether reduced apoptosis in T_{regs} was completely attributed to decreased FasL expression, or whether these cells also have intrinsic reduced sensitivity to Fas-mediated apoptosis. We directly crosslinked the Fas molecule using plate-bound α-Fas antibody to induce Fas-mediated apoptosis. Both T_{regs} and *in vitro* T_{regs} showed significantly reduced apoptosis upon direct Fas crosslinking, independent of reduced FasL expression (Figure 4d).

RICD resistance is partially dependent on soluble TGF-β1 in T_{regs}

Next we determined whether a soluble factor might influence RICD resistance in T_{cons} and T_{regs}. Therefore, we stimulated T_{cons} and T_{regs}, and collected the supernatants from 4-day cultures. We then induced RICD in the presence of T_{con} or T_{reg} supernatants. T_{reg} supernatants partially, but significantly, reduced T_{con} apoptosis (Figure 5a). We reasoned that IL-10,[36] IL-35,[37] or TGF-β,[38] the most prominent soluble factors produced by T_{regs}, may underlie apoptosis resistance, and sought to test this hypothesis. However, *Il10*$^{-/-}$ T_{regs} were as resistant to RICD as WT T_{regs} (Figure 5b). Excluding the role of IL-35 in T_{reg} survival, the frequency of Foxp3^{+} T_{regs} was normal in *Ebi3*$^{-/-}$ mice (Supplementary Figure S5). Although previous studies reported the role of TGF-β in Foxp3 expression and the development of T_{regs},[39] its effect on T_{reg} RICD is undetermined. Based on the antiapoptotic functions of TGF-β in general,[40] we examined the role of TGF-β during RICD. We either added TGF-β only during induction of RICD in T_{cons} or preconditioned them with TGF-β both during the initial stimulation and again during RICD induction. TGF-β reduced RICD moderately but significantly when added only during RICD induction (Figure 5c). However, preconditioning with TGF-β completely abrogated RICD (Figure 5c), and also induced Foxp3 expression (*in vitro* T_{regs}) in naive T cells. To confirm the role of TGF-β in conferring resistance to RICD in T_{regs}, we preblocked TGF-β (1d11 antibody) in T_{cons} and T_{regs} during primary stimulation and RICD induction. Blocking TGF-β abrogated RICD resistance partially but significantly in T_{regs} (Supplementary Figure S6). Similar to T_{regs} and consistent to a previous publication, *in vitro* T_{regs} also showed decreased apoptosis (Figure 5d).[24] Although TGF-β did not inhibit proliferation in *in vitro* T_{regs}, these cells also showed reduced active caspase levels compared with T_{cons} upon RICD induction (Supplementary Figure S7A,B). Taken together, these results show that TGF-β plays a crucial role in reducing TCR-induced RICD.

Absence of TGF-β signaling sensitizes T_{regs} to TCR-mediated RICD

Based on the antiapoptotic effects of TGF-β1 that we observed above, we hypothesized that T_{regs} resist RICD because they produce TGF-β1 and are exposed to self-stimulatory TGF-β1 signaling. To determine whether T_{regs} and *in vitro* T_{regs} exhibit increased TGF-β1 signaling, we measured the mothers against decapentaplegic homolog (SMAD) proteins.[41] Both T_{regs} and *in vitro* T_{regs} exhibited increased levels of phosphorylated SMAD2 (pSMAD2) (Figure 6a, upper panel) and pSMAD3 (Figure 6a, lower panel), whereas only a fraction of T_{cons} showed very low levels of these molecules (Figure 6a). To conclusively show that TGF-β1 signaling is required for RICD resistance of T_{regs} and *in vitro* T_{regs}, we utilized the transgenic mice that express a dominant-negative form of the TGF-β receptor II under the direction of the mouse CD4 antigen promoter (*Cd4-tgfβr2dn*^{tg}), in which CD4 cells lack TGF-β signaling.[42] We flow cytometrically sorted $CD4^+CD25^-CD44^{lo}$ naive cells and $CD4^+CD25^+T_{reg}$ cells from WT or *Cd4-tgfβr2dn*^{tg} to induce RICD. T_{regs} from WT and *Cd4-tgfβr2dn*^{tg} mice were respectively ~92 and 80% Foxp3-positive before RICD induction (Supplementary Figure S8A). We found that *Cd4-tgfβr2dn*^{tg} T_{cons} underwent RICD similar to WT T_{cons}, and both WT T_{regs} and WT *in vitro* T_{regs} showed reduced apoptosis compared with T_{cons} (Figure 6b). In striking contrast, *Cd4-tgfβr2dn*^{tg} T_{regs} and *Cd4-tgfβr2dn*^{tg} naive cells stimulated under iT_{reg} conditions (that did not upregulate Foxp3) showed increased RICD comparable to T_{cons} (Figure 6b and Supplementary Figure S8B). These data demonstrate that T_{regs} show increased TGF-β signaling, and that is central to their RICD resistance.

Expression profiles of apoptosis-related molecules in T_{regs}

Next we profiled a panel of apoptosis-related genes using quantitative PCR array analysis of messenger RNA (mRNA) isolated from T_{cons} and T_{regs} 3 h after induction of RICD. *Il10* was used as a positive control for T_{regs}. As expected, whereas mRNA level of *Il10* was upregulated, *Fasl* level was downregulated in T_{regs} (Figure 7a). Some of the Bcl-2 members such as Bcl-2 and Bcl-xl (Bcl2l1) were unchanged or moderately changed compared with T_{cons}. However, we found that antiapoptotic *Cflip (Cflar)* mRNA level was upregulated, and proapoptotic *Bax* and *Bok* were downregulated in T_{regs} compared with T_{cons}. cFLIP is a cytoplasmic protein that is capable of binding to FADD (Fas-associated death domain) and preventing the initiation of the Fas death pathway.[43] More importantly, TGF-β has previously been shown to upregulate cFLIP in other cell types.[40] Therefore, we validated the expression profiles of cFLIP and other apoptotic genes by assessing their protein levels. Although T_{regs} and *in vitro* T_{regs} upregulated Bcl-2, Bcl-xl, and Bim, their levels were slightly lower, or unchanged, compared with T_{cons} (Figure 7b). However, supporting our quantitative PCR array data, T and *in vitro* T_{regs} showed increased frequency of $cFLIP^{high}$ cells, whereas most of the T_{cons} were $cFLIP^{low}$ (Figure 7b). These results suggest that TGF-β1-mediated upregulation of cFLIP may also be involved in T_{regs} and *in vitro* T_{regs} in conferring resistance to RICD.

WT but not *Cd4-tgfβr2dn^{tg}* T_{regs} undergo reduced apoptosis during oral *Candida* reinfection *in vivo*

To determine whether increased viability of T_{regs} during the OPC infection was dependent on TGF-β, we adoptively transferred WT or *Cd4-tgfβr2dn^{tg}* $CD4^+$ cells into *Rag1$^{-/-}$* mice and assessed their viability as in Figure 1 in draining lymph nodes. We also examined the CD4 viability in mouse oral intraepithelial and lamina propria leukocytes isolated from oral tissues, the site of infection. The proportion of VD-ef660$^+$ dead cells was significantly lower among WT Foxp3$^+$ T_{regs} than in WT Foxp3$^-$ effector cells (Figure 8a,b). However, in mice that received *Cd4-tgfβr2dn^{tg}* $CD4^+$ cells, cell death of the Foxp3$^+$ T_{regs} was higher than WT T_{regs} (Figure 8a,b). We then determined the frequency of $CD25^+$ Foxp3$^+$ T_{regs} 2 days after reinfection and found that *Cd4-tgfβr2dn^{tg}* recipient mice showed at least 50% reduced frequency of Foxp3$^+$$T_{regs}$ than WT recipients (Figure 8c,d). These results demonstrate that T_{regs} resist apoptosis during later phases of infection and reinfection, and require TGF-β1 signaling for their increased viability.

DISCUSSION

Our data reveal that during late points of OPC infection (Figure 1) and chronic LCMV infection (Supplementary Figure S2), T_{regs} are exquisitely resistant to apoptosis as compared with conventional $CD4^+$ T cells. During initial phases of acute OPC infection, there was a slight drop in T_{reg} frequencies. This is consistent with a previous observation that demonstrated an infection-induced partial loss of T_{regs} because of insufficiency in IL-2.[44] However, at late time points, whereas most of the effector cells undergo attrition, T_{regs} survive RICD. We and others have shown that during infections, Toll-like receptor-2 signaling can promote proliferation and accumulation of T_{regs} in the infected tissues and the draining lymph nodes, and is required to limit immunopathology.[31,45] Although T_{regs} underwent proliferation, their expansion is less than that of the effector cells, and could not have contributed to increased viability compared with effector cells (Supplementary Figure S1A). It is conceivable that although most effector cells die after infection clearance, T_{regs} have adopted a survival mechanism to be retained longer in the tissues and limit inflammation and tissue damage. This is consistent to the previous data showing that memory T_{regs} stay in the system, and serve as more potent suppressors mediating resolution of organ-specific autoimmunity in mice.[46]

Our data unequivocally show that TGF-β1 is required for RICD resistance in T_{regs}. Addition of exogenous T_{reg} supernatant or TGF-β1 partially relieved even the T_{con} cells from RICD (Figure 5a), demonstrating a partial role of soluble TGF-β1 in decreasing apoptosis during RICD. Moreover, *Cd4-tgfβr2dn^{tg}* T_{regs} showed complete susceptibility to RICD similar to T_{con} levels, substantiating a critical role of TGF-β1 signaling in T_{reg} RICD resistance (Figure 6b). We have shown for the first time that TGF-β1 confers increased viability in T_{regs} at the site of infection (mouse oral intraepithelial and lamina propria leukocyte tissue) during an oral infection *in vivo* (Figure 8a), phenotypically and mechanistically recapitulating the *in vitro* results. It is possible that both soluble TGF-β1 and membrane-bound TGF-β1 (latency-associated peptide) are jointly involved in apoptosis resistance in T_{regs}. Thus, in the absence of TGF-βRII, unable to respond to both the forms of TGF-β, T_{regs}

showed high susceptibility to RICD. Validating the role of TGF-β further in CD4 cells, TGF-β1-induced *in vitro* T_{regs} exhibited RICD resistance as well. Because *in vitro* T_{regs} express Foxp3, it can be argued that Foxp3 imparts increased viability in T_{regs}.[27] However, our results showing high RICD susceptibility of FACS-sorted T_{regs} from *Cd4-tgfβr2dn*^{tg} mice despite Foxp3 expression (Supplementary Figure S8B) rules out this possibility. A potential caveat to the experiment where we adoptively transferred *Cd4-tgfβr2dn*^{tg} T_{regs} could be the loss of Foxp3 expression in some of the T_{regs}. Moreover, as we purified these cells using CD4 and CD25 only, there is likely a contamination of CD25$^+$ T_{eff} cells. However, in our viability analyses we gated only on Foxp3$^+$ T_{regs} (Figure 8a). Therefore, although the starting populations may have been different in terms of Foxp3 expression, even gating exclusively on Foxp3 + T_{regs}, *Cd4-tgfβr2dn*^{tg} T_{regs} had poor viability. These results show that despite Foxp3 expression in *Cd4-tgfβr2dn*^{tg} cells, they have poor survival, thus substantiating the role of TGF-β in maintaining T_{reg} survival. Moreover, the overall viable CD4 count of the cells recovered from CLN showed that *Cd4-tgfβr2dn*^{tg} CD4 cell recipient mice had lower CD4 cell numbers than the WT CD4 cell recipients on day 2 after reinfection (Supplementary Figure S9). These results show that *Cd4-tgfβr2dn*^{tg} CD4 + cells did not expand better than WT CD4 T cells at this time point. Therefore, decrease in Foxp3$^+$ cells in Figure 8c,d could not be because of preferential expansion of the activated cell population (Foxp3 negative) on day 2 at which we measured the frequency of Foxp3$^+$ cells.

Thus, we believe that TGF-β1 can confer RICD resistance independently of Foxp3 expression. As shown previously,[27] although we observed lower FasL expression in T_{regs} and *in vitro* T_{regs} compared with T_{cons} (Figures 4b, 7a), we do not attribute the RICD resistance of T_{regs} solely to reduced FasL expression. This is because human T_{regs} show little or no reduction in FasL expression compared with T_{cons} (data not shown),[47] yet are resistant to RICD (Figure 2e,f). Moreover, in contrast to the previous findings in naive T_{regs},[48] activated T_{regs} and *in vitro* T_{regs} showed increased apoptosis resistance even to intrinsic Fas apoptosis that was induced directly using α-FAS antibody (Figure 4d).

We believe that TGF-β1 is involved in cFLIP upregulation in T_{regs} and *in vitro* T_{regs} (Figure 7b), based on a previous study that demonstrated cFLIP induction by TGF-β.[40] When we stimulated naive cells using α-CD3 antibody in the presence of IL-2 and TGF-β, the naive T cells not only expressed Foxp3 and became *in vitro* T_{regs}, but they also expressed higher levels of cFLIP compared with cells without TGF-β (Figure 7b). These results show that TGF-β is involved in inducing cFLIP along with Foxp3 expression in naive T cells. cFLIP may inhibit intrinsic Fas signaling, contributing to FasL-independent component of RICD resistance in T_{regs}. Future studies are warranted to investigate cFLIP-dependent survival in T_{regs} during infections. Thus, our data not only support the previously demonstrated role of TGF-β1 in inducing T_{regs} and controlling inflammation,[39] but also reveal its role in promoting T_{reg} resistance to Fas-dependent RICD *in vitro* and during infections. Taken together, we show that TGF-β1 contributes to apoptosis resistance mechanism to T_{regs} and *in vitro* T_{regs} during RICD that has implications in controlling immunopathology during microbial infections.

METHODS

Antibodies, reagents, and mice

Purified and fluorochrome-conjugated CD3 (145-2C11), CD28, CD25 (3C7), CD4, Foxp3, and p-Akt antibodies were purchased from eBiosciences (San Diego, CA). Fluorochrome-conjugated annexin-V, Bcl-2, Fas, FasL, Bcl-xl, and Bim antibodies were all purchased from BD Biosciences (San Diego, CA). cFLIP, cleaved caspase-3, caspase-9, and pAkt antibodies were purchased from Cell Signaling Technologies (Danvers, MA). FasL blocking antibody was purchased from R&D Systems (Minneapolis, MN). Fas crosslinking antibody was purchased from Alexis Biochemicals (Farmingdale, NY). Antibody to NF-κB (p65) was purchased from Santa Cruz Biotechnology (Santa Cruz, CA). Mouse CD4 isolation kits were purchased from Miltenyi Biotec (Auburn, CA) or from Stem Cell Technologies (Vancouver, BC, Canada). Mouse IL-2, IL-10, and human TGF-β were purchased from R&D Systems and BioBasic (Amherst, NY). Complete RPMI-1640 (Hyclone, GE Healthcare, Pittsburgh, PA) supplemented with 10% fetal bovine serum, 100 U ml^{-1} penicillin (BioBasic), 100 μg ml^{-1} streptomycin (BioBasic), 1× Glutamax (Gibco, Thermo Fisher Scientific, Grand Island, NY), and 50 μM β-mercaptoethanol was used for cell cultures. $Foxp3^{GFP}$ reporter mice on Balb/C or C57BL/6 background, and $Foxp3^{YFPcre}$, *Rag1*$^{-/-}$, *Il10*$^{-/-}$ *Ebi3*$^{-/-}$, and *Cd4-tgfβr2dn*^{tg} mice and the appropriate control mice were purchased from Jackson Laboratories (Bar Harbor, ME). Experiments were performed at Case Western Reserve University (CWRU) in compliance with the CWRU School of Medicine Institutional Animal Care and Use Committee, and adhered to national guidelines published in Guide for the Care and Use of Laboratory Animals, 8th Edn, National Academies Press, 2001(protocol no. 2012-0140). Human cells were obtained from peripheral blood mononuclear cells of the healthy donors obtained under an approved protocol, reviewed, and approved by the University Hospitals Case Medical Center institutional review board (protocol no. 03-13-15). All subjects provided written informed consent, and participants <18 years of age were not enrolled in the study.

RICD induction in mouse and human CD4 cells *in vitro*

$CD4^+CD25^+Foxp3^{GFP+}$ T_{regs} or $CD4^+CD44^{low}$ $CD25^-$ $Foxp3^{GFP-}$ naive T cells (T_{con}) were isolated from $Foxp3^{GFP}$ reporter mice and cultured in flat-bottom 96-well plates in the presence of soluble 1 μg ml^{-1} α-CD3 and 2 μg ml^{-1} α-CD28 antibodies and human IL-2 (10 ng ml^{-1}). For induction of T_{regs} *in vitro* human TGF-β1 (4 ng ml^{-1}) was added to naive cells during the primary stimulation. After 4–5 days, dead cells were removed using Ficoll-Paque centrifugation, and restimulated with plate-bound α-CD3 antibody and IL-2 (10 ng ml^{-1}) for RICD induction. Where indicated, cells were labeled with cell proliferation dye- 670 (CPD670) at the beginning of stimulation. For some experiments, $CD4^+CD25^+$ T_{regs} and $CD4^+CD44^{low}$ $CD25^-$ T_{cons} were isolated. For human cell experiments, $CD4^+CD25^{hi}$ $CD127^{lo}$ T_{regs} and $CD4^+$ $CD44^{low}CD25^-$ T_{cons} were used for initial stimulation with 1 μg ml^{-1} α-CD3 (OKT3) and 2 μg ml^{-1} α-human CD28 antibodies. After 5 days, RICD was induced using plate-bound OKT3 antibody and IL-2.

Measurement of cell viability by flow cytometry

Cell viability was examined on the basis of forward scatter (FSC) or annexin-V and PI staining of the cells from triplicate culture wells. The percentage of annexin-V^+PI^+ or FSC^{lo} PI^+ in flow cytometric plots was used as frequency of dead cells to calculate percentage apoptosis (% Apoptosis). % Apoptosis plotted in all analyses is normalized to the cultures that were stimulated with 0 μg ml^{-1} α-CD3 antibody, whose cell death was set at 0%. In some experiments, where intracellular Foxp3 expression was also determined, we measured the viability of $CD4^+$ cells using viability dye-efluor660 (VD-ef660, eBiosciences, San Diego, CA). Data were acquired using BD FACS Calibur or BD LSR Fortessa (Franklin Lakes, NJ) analyser cytometers and were analyzed using FlowJo 9.8 software (Tree Star, Ashland, OR).

NF-κB nuclear translocation

After 30-min restimulation, cells were collected for fixation and permeabilization. To determine the nuclear translocation of the NF-κB, cells were cytospun down on the slides, stained using α-p65 antibody, and were assessed by confocal microscopy.

Apoptosis induction *in vivo* by administration of α-CD3 antibody in mice

$Foxp3^{GFP}$ reporter mice were injected with phosphate-buffered saline or 100 μg of α-CD3 antibody (eBiosciences) by intraperitoneal injection. At 1 day after injection, mice were killed, the spleen and lymph nodes were isolated in single-cell suspensions, and the viability of the cells was assayed using green fluorescent protein (GFP) and PI staining and flow cytometry.

Quantitative reverse transcriptase-PCR array analysis

RT^2 Profiler PCR array plates (PAMM-012Z) from Qiagen/SABiosciences (Valencia, CA) were used for profiling apoptosis-related mRNA expression according to the manufacturer's instructions. Arrays contained 84 apoptosis-related genes and 12 housekeeping genes. T_{regs} or T_{cons} were harvested 1 h after RICD stimulation, and RNA was recovered using an EZ-10 RNA isolation kit (BioBasic). Genomic DNA was removed by DNA Away (Ambion; Life Technologies (Grand Island, NY; AM1906)) and complementary DNA was synthesized from total RNA using MuLV reverse transcriptase enzyme (BioBasic) with OligodT primers. Then, 1 μl of complementary DNA was used per array well in one reaction using the SYBR Green quantitative PCR reaction in a real-time PCR machine ABI7900HT (Applied Biosystems, Grand Island, NY).

Oral *Candida* infection in mice

Mice were infected as previously described.[30,49] Briefly, they were sublingually infected under anesthesia by placing a 3 mm diameter cotton ball saturated with 1×10^8 *Candida albicans* (CAF2-1) blastospores for 90 min. For experiments involving adoptive transfer of cells, $Rag1^{-/-}$ mice were reconstituted with indicated congenic cells 3–4 days before infection. Mice were reinfected on day 5 after primary infection for assessing the viability during RICD *in vivo*.

LCMV infection in mice

Foxp3^{YFP} reporter mice were obtained from Jackson Laboratory and were infected intravenously with 2×10^6 PFUs of the LCMV clone 13. Virus was diluted in 200 μl phosphate-buffered saline and injected via retro-orbital route in mice anesthetized with isoflurane. Viral stocks were prepared and viral titers were measured as previously described.[50]

Statistical analyses

Statistical significance and *P*-values were determined by Mann–Whitney tests in Prism 6.0 (GraphPad Software, La Jolla, CA). The s.d. values are shown in the data unless otherwise specified.

Supplementary Material

Refer to Web version on PubMed Central for supplementary material.

Acknowledgments

We thank Case Comprehensive Cancer center flow cytometry core facility for assisting in FACS cell purification, and access to CFAR flow cytometry core analyzers. P.P. was supported by departmental startup funds from the School of Dental Medicine. This work was also supported by a CTSC core utilization grant to P.P. and SDRC P30AR039750 grant to D.P.

References

1. Pandiyan P, Zheng L, Lenardo MJ. The molecular mechanisms of regulatory T cell immunosuppression. Front Immunol. 2011; 2:60. [PubMed: 22566849]
2. Sakaguchi S, Yamaguchi T, Nomura T, Ono M. Regulatory Tcells and immune tolerance. Cell. 2008; 133:775–787. [PubMed: 18510923]
3. Cebula A, et al. Thymus-derived regulatory T cells contribute to tolerance to commensal microbiota. Nature. 2013; 497:258–262. [PubMed: 23624374]
4. Miyara M, Gorochov G, Ehrenstein M, Musset L, Sakaguchi S, Amoura Z. Human FoxP3+ regulatory T cells in systemic autoimmune diseases. Autoimmun Rev. 2011; 10:744–755. [PubMed: 21621000]
5. Whiteside TL. Regulatory T cell subsets in human cancer: are they regulating for or against tumor progression? Cancer Immunol Immunother. 2014; 63:67–72. [PubMed: 24213679]
6. Shi LZ, et al. Inhibitory role of the transcription repressor Gfi1 in the generation of thymus-derived regulatory Tcells. Proc Natl Acad Sci USA. 2013; 110:E3198–E3205. [PubMed: 23918371]
7. Pierson W, et al. Antiapoptotic Mcl-1 is critical for the survival and niche-filling capacity of Foxp3(+) regulatory T cells. Nat Immunol. 2013; 14:959–965. [PubMed: 23852275]
8. Lenardo MJ. Molecular regulation of T lymphocyte homeostasis in the healthy and diseased immune system. Immunol Res. 2003; 27:387–398. [PubMed: 12857983]
9. Snow AL, Pandiyan P, Zheng L, Krummey SM, Lenardo MJ. The power and the promise of restimulation-induced cell death in human immune diseases. Immunol Rev. 2010; 236:68–82. [PubMed: 20636809]
10. Hildeman DA, et al. Activated Tcell death in vivo mediated by proapoptotic bcl-2 family member bim. Immunity. 2002; 16:759–767. [PubMed: 12121658]
11. Marrack P, Kappler J. Control of Tcell viability. Annu Rev Immunol. 2004; 22:765–787. [PubMed: 15032596]
12. Russell JH, White CL, Loh DY, Meleedy-Rey P. Receptor-stimulated death pathway is opened by antigen in mature T cells. Proc Natl Acad Sci USA. 1991; 88:2151–2155. [PubMed: 1826050]

13. Schmitz I, Krueger A, Baumann S, Schulze-Bergkamen H, Krammer PH, Kirchhoff S. An IL-2-dependent switch between CD95 signaling pathways sensitizes primary human T cells toward CD95-mediated activation-induced cell death. J Immunol. 2003; 171:2930–2936. [PubMed: 12960316]
14. Hildeman DA, Zhu Y, Mitchell TC, Kappler J, Marrack P. Molecular mechanisms of activated Tcell death in vivo. Curr Opin Immunol. 2002; 14:354–359. [PubMed: 11973134]
15. Bidere N, Su HC, Lenardo MJ. Genetic disorders of programmed cell death in the immune system. Annu Rev Immunol. 2006; 24:321–352. [PubMed: 16551252]
16. Duke RC, Cohen JJ. IL-2 addiction: withdrawal of growth factor activates a suicide program in dependent Tcells. Lymphokine Res. 1986; 5:289–299. [PubMed: 2946903]
17. Strasser A. The role of BH3-only proteins in the immune system. Nat Rev Immunol. 2005; 5:189–200. [PubMed: 15719025]
18. Strasser A, O'Connor L, Dixit VM. Apoptosis signaling. Annu Rev Biochem. 2000; 69:217–245. [PubMed: 10966458]
19. Pandiyan P, Lenardo MJ. The control of CD4+CD25+Foxp3+ regulatory T cell survival. Biol Direct. 2008; 3:6. [PubMed: 18304352]
20. Barron L, et al. Cutting edge: mechanisms of IL-2-dependent maintenance of functional regulatory T cells. J Immunol. 2010; 185:6426–6430. [PubMed: 21037099]
21. Rathmell JC, Thompson CB. Pathways of apoptosis in lymphocyte development, homeostasis, and disease. Cell. 2002; 109:S97–S107. [PubMed: 11983156]
22. Chaudhry A, Rudensky AY. Control of inflammation by integration of environmental cues by regulatory T cells. J Clin Invest. 2013; 123:939–944. [PubMed: 23454755]
23. Weant AE, Michalek RD, Crump KE, Liu C, Konopitski AP, Grayson JM. Defects in apoptosis increase memory CD8+ T cells following infection of Bim−/−Faslpr/lpr mice. Cell Immunol. 2011; 271:256–266. [PubMed: 21839428]
24. Tischner D, Wiegers GJ, Fiegl H, Drach M, Villunger A. Mutual antagonism of beta and Interleukin-2 in cell survival and lineage commitment of induced regulatory T cells. Cell Death Differ. 2012; 19:1277–1287. [PubMed: 22322859]
25. Ouyang W, Beckett O, Ma Q, Li MO. Transforming growth factor-beta signaling curbs thymic negative selection promoting regulatory T cell development. Immunity. 2010; 32:642–653. [PubMed: 20471291]
26. Banz A, Pontoux C, Papiernik M. Modulation of Fas-dependent apoptosis: a dynamic process controlling both the persistence and death of CD4 regulatory Tcells and effector Tcells. J Immunol. 2002; 169:750–757. [PubMed: 12097377]
27. Weiss EM, et al. Foxp3-mediated suppression of CD95L expression confers resistance to activation-induced cell death in regulatory T cells. J Immunol. 2011; 187:1684–1691. [PubMed: 21746966]
28. Rowe JH, Ertelt JM, Way SS. Foxp3(+) regulatory T cells, immune stimulation and host defence against infection. Immunology. 2012; 136:1–10. [PubMed: 22211994]
29. Zhou Y. Regulatory T cells and viral infections. Front Biosci. 2008; 13:1152–1170. [PubMed: 17981620]
30. Pandiyan P, et al. CD4(+)CD25(+)Foxp3(+) regulatory T cells promote Th17 cells *in vitro* and enhance host resistance in mouse Candida albicans Th17 cell infection model. Immunity. 2011; 34:422–434. [PubMed: 21435589]
31. Bhaskaran N, Weinberg A, Pandiyan P. Th17 inflammation model of oropharyngeal candidiasis in immunodeficient mice. J Vis Exp. 2015; 96:52538.
32. Filler SG, Yeaman MR, Sheppard DC. Tumor necrosis factor inhibition and invasive fungal infections. Clin Infect Dis. 2005; 41(Suppl 3):S208–S212. [PubMed: 15983902]
33. Hughes PD, Belz GT, Fortner KA, Budd RC, Strasser A, Bouillet P. Apoptosis regulators Fas and Bim cooperate in shutdown of chronic immune responses and prevention of autoimmunity. Immunity. 2008; 28:197–205. [PubMed: 18275830]
34. Yu XZ, Zhu L, Davis JE, Tso JY, Hansen JA, Anasetti C. Induction of apoptosis by anti-CD3 epsilon F(ab')2 in antigen receptor transgenic murine T cells activated by specific peptide. J Immunol. 1996; 157:3420–3429. [PubMed: 8871640]

35. Lenardo MJ. Interleukin-2 programs mouse alpha beta T lymphocytes for apoptosis. Nature. 1991; 353:858–861. [PubMed: 1944559]
36. Ina K, et al. Intestinal fibroblast-derived IL-10 increases survival of mucosal T cells by inhibiting growth factor deprivation- and Fas-mediated apoptosis. J Immunol. 2005; 175:2000–2009. [PubMed: 16034145]
37. Collison LW, Pillai MR, Chaturvedi V, Vignali DA. Regulatory T cell suppression is potentiated by target T cells in a cell contact, IL-35- and IL-10-dependent manner. J Immunol. 2009; 182:6121–6128. [PubMed: 19414764]
38. Wan YY, Flavell RA. Regulatory T cells, transforming growth factor-beta, and immune suppression. Proc Am Thorac Soc. 2007; 4:271–276. [PubMed: 17607012]
39. Marie JC, Letterio JJ, Gavin M, Rudensky AY. TGF-beta1 maintains suppressor function and Foxp3 expression in CD4+CD25+ regulatory T cells. J Exp Med. 2005; 201:1061–1067. [PubMed: 15809351]
40. Schlapbach R, et al. TGF-beta induces the expression of the FLICE-inhibitory protein and inhibits Fas-mediated apoptosis of microglia. Eur J Immunol. 2000; 30:3680–3688. [PubMed: 11169411]
41. Kamato D, et al. Transforming growth factor-beta signalling: role and consequences of Smad linker region phosphorylation. Cell Signal. 2013; 25:2017–2024. [PubMed: 23770288]
42. Gorelik L, Flavell RA. Abrogation of TGFbeta signaling in Tcells leads to spontaneous T cell differentiation and autoimmune disease. Immunity. 2000; 12:171–181. [PubMed: 10714683]
43. Yeh WC, et al. Requirement for Casper (c-FLIP) in regulation of death receptor-induced apoptosis and embryonic development. Immunity. 2000; 12:633–642. [PubMed: 10894163]
44. Benson A, et al. Microbial infection-induced expansion of effector T cells overcomes the suppressive effects of regulatory T cells via an IL-2 deprivation mechanism. J Immunol. 2012; 188:800–810. [PubMed: 22147768]
45. Bhaskaran N, Cohen S, Zhang Y, Weinberg A, Pandiyan P. TLR-2 signaling promotes IL-17A production in CD4+CD25+Foxp3 regulatory cells during oropharyngeal Candidiasis. Pathogens. 2015; 4:90–110. [PubMed: 25790134]
46. Rosenblum MD, Gratz IK, Paw JS, Lee K, Marshak-Rothstein A, Abbas AK. Response to self antigen imprints regulatory memory in tissues. Nature. 2011; 480:538–542. [PubMed: 22121024]
47. Baatar D, Olkhanud P, Sumitomo K, Taub D, Gress R, Biragyn A. Human peripheral blood T regulatory cells (Tregs), functionally primed CCR4 + Tregs and unprimed CCR4- Tregs, regulate effector Tcells using FasL. J Immunol. 2007; 178:4891–4900. [PubMed: 17404270]
48. Fritzsching B, et al. Naive regulatory Tcells: a novel subpopulation defined by resistance toward CD95L-mediated cell death. Blood. 2006; 108:3371–3378. [PubMed: 16868256]
49. Kamai Y, Kubota M, Kamai Y, Hosokawa T, Fukuoka T, Filler SG. New model of oropharyngeal candidiasis in mice. Antimicrob Agents Chemother. 2001; 45:3195–3197. [PubMed: 11600377]
50. Popkin DL, et al. Hypomorphic mutation in the site-1 protease Mbtps1 endows resistance to persistent viral infection in a cell-specific manner. Cell Host Microbe. 2011; 9:212–222. [PubMed: 21402360]

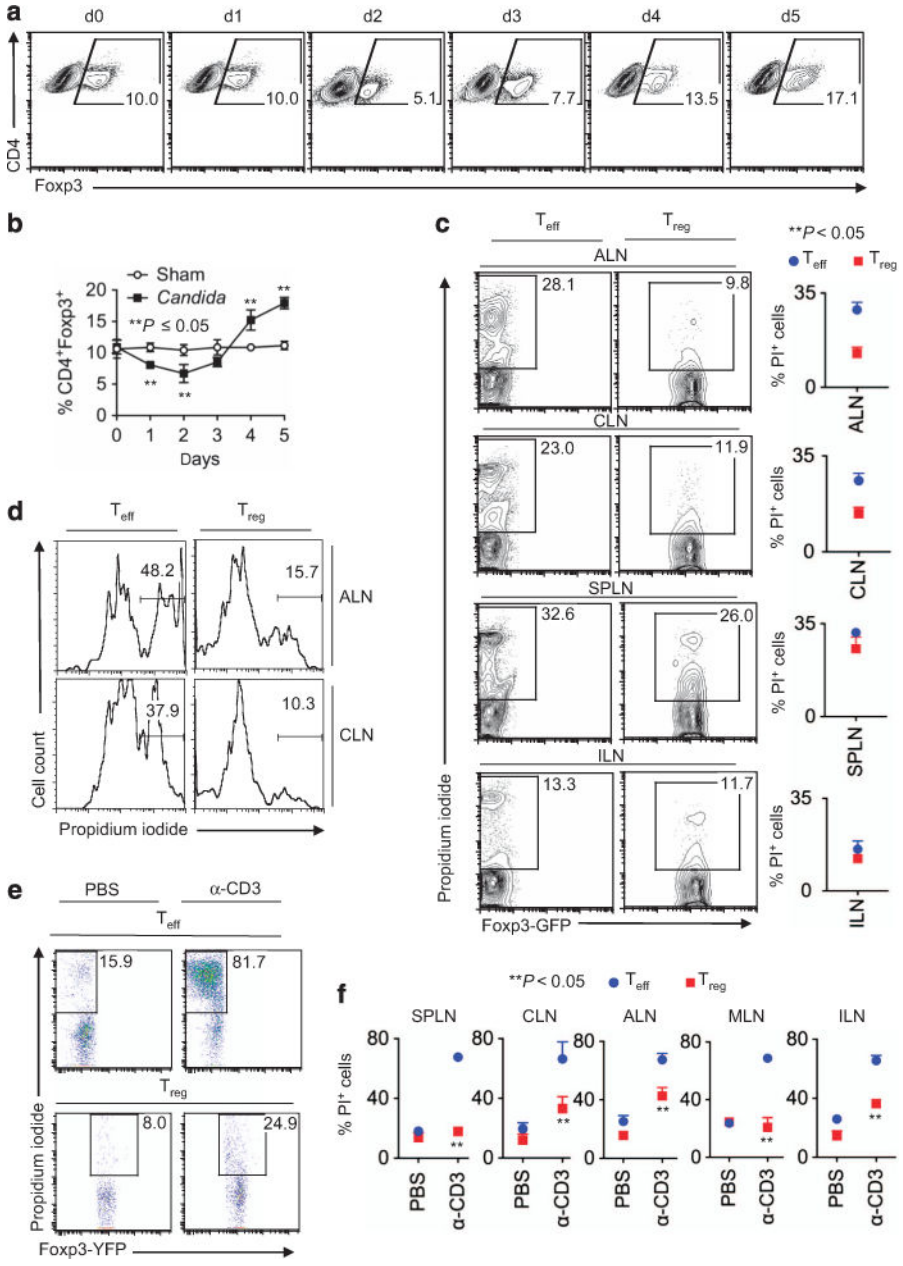

Figure 1.

Regulatory T cells (T_{regs}) show increased viability during *Candida* reinfection and *in vivo*. (**a, b**) $CD4^+Foxp3^+$ T_{regs} show increased enrichment during the course of oropharyngeal candidiasis (OPC) in mice. $Foxp3^{GFP}$ reporter mice (n = 5/group) were infected with *Candida albicans* (*Candida*) as described in Methods. Flow cytometric plots (**a**) and statistical analyses (**b**) showing the frequencies of cells expressing CD4 and intracellular Foxp3 (gated on CD4 cells) in cervical lymph nodes (CLNs) at various days (d) after *C. albicans* infection. Percentages of Foxp3-expressing cells are shown. *P*-value is determined by Mann–Whitney test. (**c**) Mice were infected and reinfected as in **a**. Axillary lymph nodes (ALNs), CLNs, spleen (SPLN), and inguinal lymph nodes (ILNs) were harvested on day 1 after reinfection to examine cell death of $Foxp3^{GFP-}$ T_{eff} (left) and $Foxp3^{GFP+}T_{regs}$ (right)

ex vivo by green fluorescent protein (GFP) and propidium iodide (PI) staining. Flow cytometric contour plots (left panel) and statistical data (right panel) show the frequencies of PI^+ cells (gated on CD4 cells). Statistical significance was determined using Mann–Whitney test. (**d**) *Rag1*$^{-/-}$ CD45.1 mice (n =5/group) were reconstituted with $CD4^+Foxp3^{GFP-}$ T_{eff} or $CD4^+Foxp3^{GFP+}T_{reg}$ cells obtained from congenic CD45.2 mice. Recipient mice in each group were reinfected with *Candida*. ALNs and CLNs were harvested on day 1 after reinfection for examining cell death *ex vivo* by PI staining (gated on $CD45.2^+$ cells). (**e, f**) $Foxp3^{GFP}$ reporter mice were injected with phosphate-buffered saline (PBS) or α-CD3 antibody. Flow contour plots of yellow fluorescent protein (YFP) and PI staining histograms (**e**) of $Foxp3^{YFP-}$ T_{eff} (top) and $Foxp3^{YFP+}$ T_{regs} (bottom) and quantification of % PI^+ cells (**f**) of $Foxp3^{GFP-}$ T_{eff} (blue circles) and $Foxp3^{YFP+}$ T_{regs} (red squares) 24 h after α-CD3 antibody injection in mice (n =4/group) (gated on $CD4^+$ cells). Statistical significance was determined using Mann–Whitney test. Data from one of three to five independent experiments are shown.

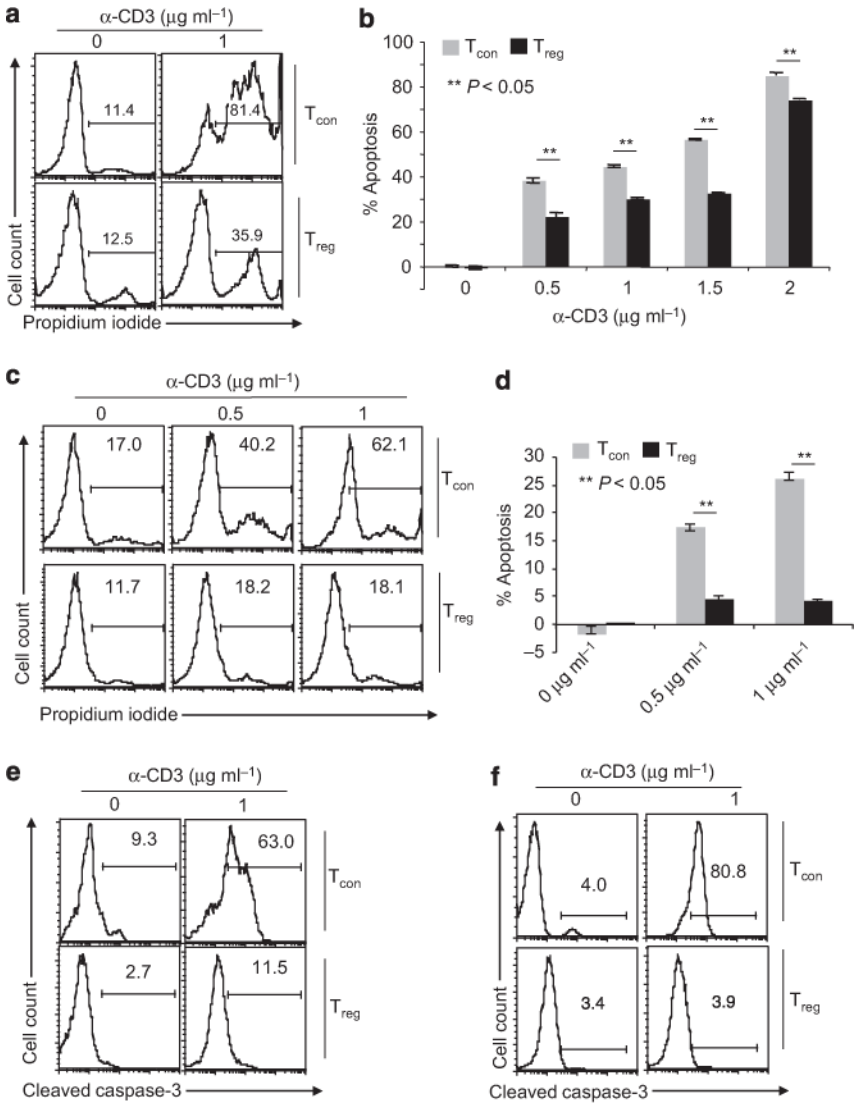

Figure 2.

Mouse and human regulatory T cells (T_{regs}) are resistant to restimulation-induced cell death (RICD) and show decreased activated caspase levels. (**a**) Flow cytometric histogram plots of propidium iodide (PI) staining of mouse T_{cons} (upper panel) and mouse T_{regs} (lower panel) derived and pooled from spleen/lymph nodes (SPLN/LN), stimulated under RICD conditions for 20 h with 0 μg ml^{-1} (left) or 1 μg ml^{-1} (right) of α-CD3 antibody. As controls, we stimulated the cells with interleukin-2 (IL-2) only, but no α-CD3 antibody (0 μg ml^{-1}). (**b**) Quantification of % apoptosis of the T_{cons} (gray bars) or T_{regs} (black bars) restimulated with indicated concentrations of α-CD3 antibody for 18 h, based on evaluating the annexin-V and PI staining by flow cytometry. (**c**) Flow cytometric analyses of PI staining of human T_{cons} (upper panel) and human T_{regs} (lower panel) stimulated under RICD conditions for 21 h with 0 μg ml^{-1} (left), 0.5 μg ml^{-1} (middle), or 1 μg ml^{-1} (right) of α-CD3 antibody. (**d**) % Apoptosis quantification of human cells stimulated as in **c**. (**e**) Mouse cells or (**f**) human cells were stimulated for 15 h as in **a** and **c**, respectively, and cleaved caspase-3 levels were determined by intracellular staining and flow cytometry. *P*-values are

determined by Mann–Whitney test in **b** and **d**. Data in **a** and **b** represent at least 10 independent experiments and in **c–f** are from one of three independent experiments showing similar results.

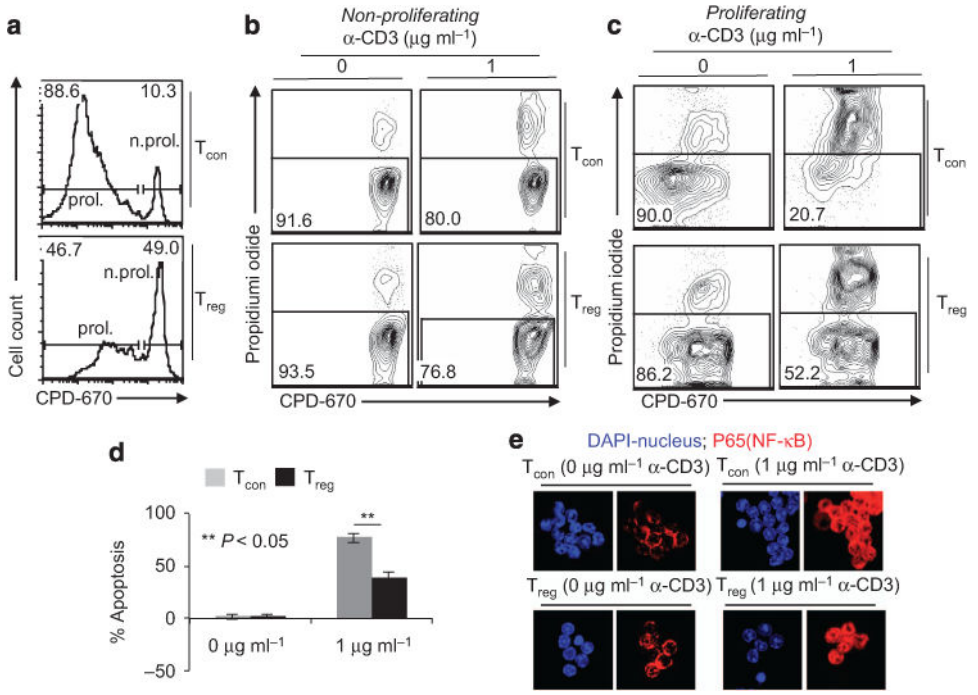

Figure 3.

Reduced restimulation-induced cell death (RICD) in regulatory T cells (T_{regs}) is not dependent on retarded proliferation or reduced activation. (**a**) Flow cytometric histogram plots showing CPD670 dilution of mouse T_{cons} (upper panel) and mouse T_{regs} (lower panel) derived and pooled from spleen/lymph nodes (SPLN/LN), sorted as described in Methods, and stimulated for 4 days with α-CD3, α-CD28, and interleukin-2 (IL-2) without RICD induction. CPD670 dilution shows the frequency of proliferating (prol.) and nonproliferating cells (n.prol.). (**b, c**) T_{con} or T_{reg} cells labeled and stimulated as in a were restimulated with (right) or without (left) 1 μg ml^{-1} of α-CD3 antibody. Flow cytometric contour plots show CPD670 dilution and propidium iodide (PI) staining of T_{con} (top) or T_{reg} (bottom) cells gated on (**b**) nonproliferating cells and (**c**) proliferating cells. Plots show the frequency of PI-negative viable cells. (**d**) Statistical representation of % apoptosis of nonproliferating cells (upper panel) and proliferating cells (lower panel). *P*-value is determined by Mann–Whitney test. Data represent one of two independent experiments showing similar results. (**e**) T_{cons} (upper panel) or T_{regs} (lower panel) were restimulated with 1 μg ml^{-1} α-CD3 or 0 μg ml^{-1} α-CD3 under RICD conditions for 30 min. Cells were fixed, stained using α-p65 antibody (red) and 6-diamidino-2-phenylindole (DAPI) (nucleus; blue), and assessed by confocal microscopy. Data from one of three independent experiments are shown.

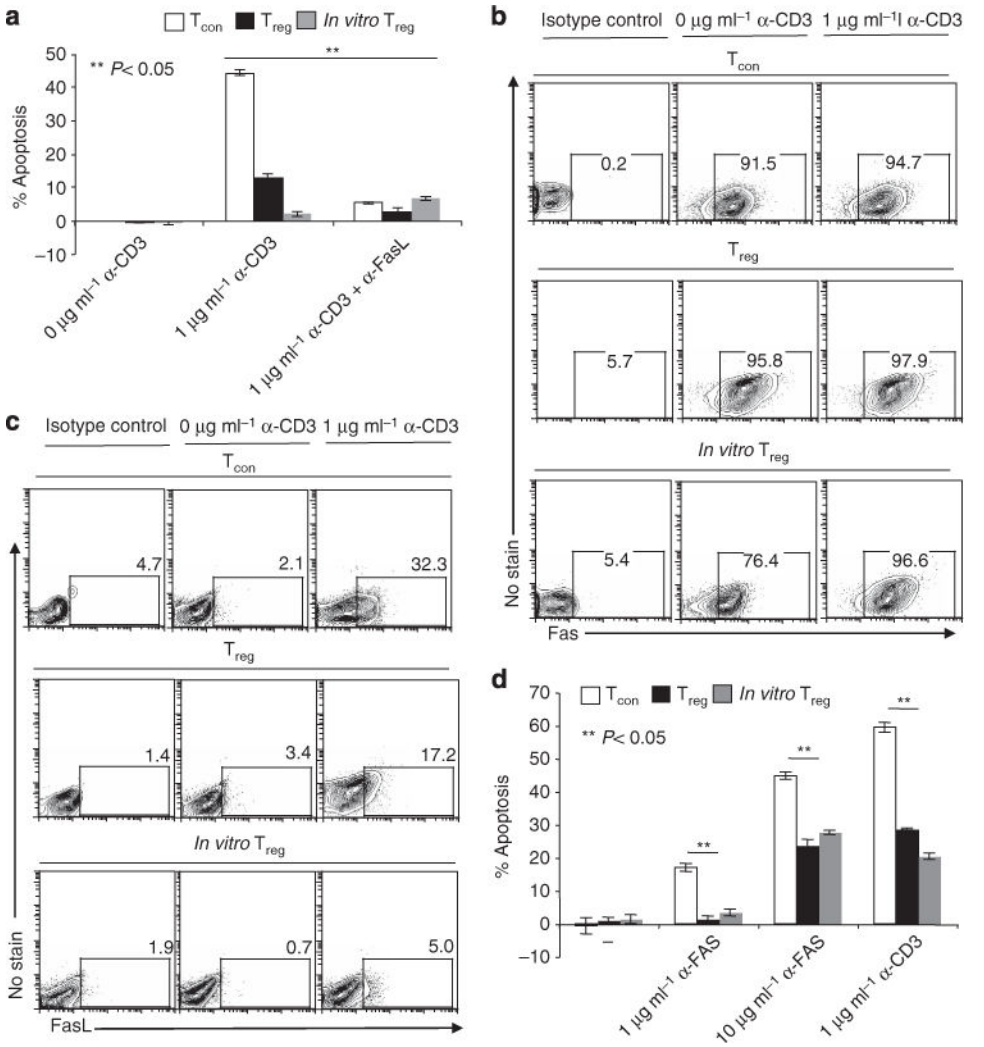

Figure 4.

Regulatory T cells (T_{regs}) and *in vitro* T_{regs} show decreased Fas ligand (FasL)/FAS mediated death. (**a**) % Apoptosis of T_{cons} (white bars), T_{regs} (black bars), or *in vitro* T_{regs} (gray bars) derived and pooled from spleen/lymph nodes (SPLN/LN) that were stimulated under restimulation-induced cell death (RICD) conditions with or without 1 μg ml^{-1} of α-CD3 antibody for 12 h, as in Figure 2b. Isotype control antibody or α-FasL antibody (10 μg ml^{-1}) was added 30 min before RICD induction. (**b, c**) Flow cytometric contour plots of Fas (**b**) or FasL (**c**) staining of T_{con} (top row), T_{reg} (middle row), or iT_{reg} (bottom row) cells, stimulated as in Figure 2b. Left columns show isotype control staining on T_{con} cells. Gates show the frequencies of Fas- or FasL-expressing cells. Data represent one of three independent experiments showing similar results. (**d**) % Apoptosis of T_{cons} (white bars), T_{regs} (black bars), or *in vitro* T_{regs} (gray bars) that were restimulated with 1 or 10 μg ml^{-1} of α-Fas antibody and human interleukin-2 (IL-2) for 8 h. As controls, some cells were restimulated with 0 or 1 μg ml^{-1} of α-CD3 antibody. *P*-values are determined by Mann–Whitney test.

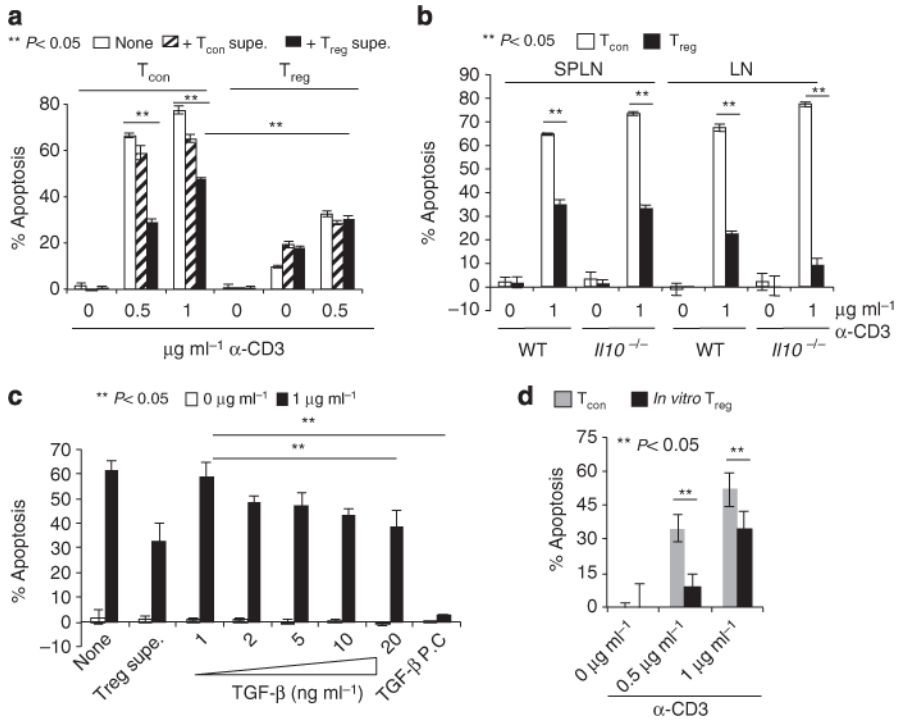

Figure 5.

Restimulation-induced cell death (RICD) in T_{cons} is partially reduced by a soluble factor secreted by regulatory T cells (T_{regs}) and the reduced apoptosis is dependent on transforming growth factor-β1 (TGF-β). (**a**) T_{cons} and T_{regs} derived and pooled from spleen/lymph nodes (SPLN/LN) were stimulated under RICD conditions for 20 h with indicated concentrations of α-CD3 antibody as in Figure 2b, in the absence (white bars) or the presence of supernatants collected from 4-day T_{con} cultures (T_{con} supe.) (hatched bars) or those collected from T_{reg} cultures (T_{reg} supe.) (black bars). % Apoptosis, as assessed by annexin-V and propidium iodide (PI) staining. (**b**) % Apoptosis of wild-type (WT) or *Il10*$^{-/-}$ T_{cons} (white bars) or T_{regs} (black bars) that were stimulated under RICD conditions for 10 h as in Figure 2b. (**c**) % Apoptosis of WT T_{cons} restimulated as in Figure 2b in the presence of T_{reg} supe., or increasing concentrations of human TGF-β1 added during RICD induction only. Some T_{cons} were cultured with 4 ng ml^{-1} of TGF-β1 during initial stimulation for 4 days (preconditioning (PC)) and during RICD. (**d**) *In vitro* T_{regs} are resistant to RICD. % Apoptosis of T_{cons} (gray bars) or *in vitro* T_{regs} (black bars) that were restimulated with indicated concentrations of α-CD3 antibody for 17 h as in Figure 2b. *P*-values are determined by Mann–Whitney test.

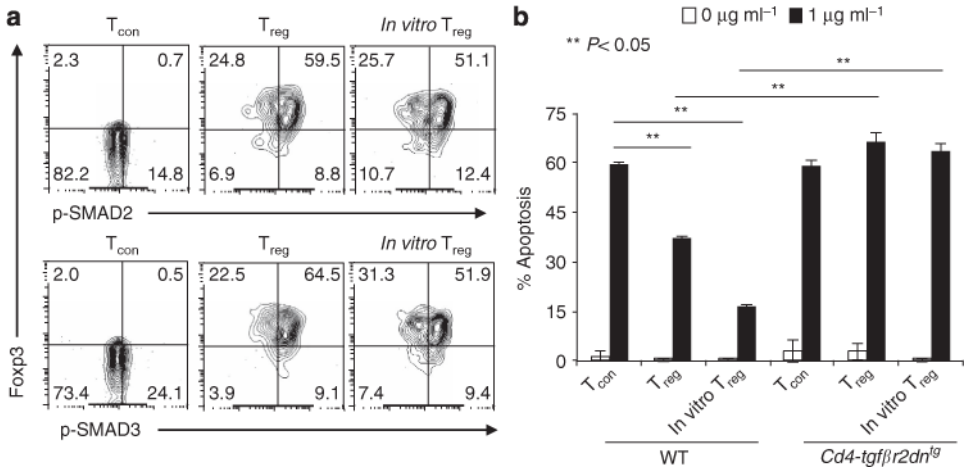

Figure 6.

Resistance to restimulation-induced cell death (RICD) is dependent on increased transforming growth factor-β1 (TGF-β1) signaling in regulatory T cells (T_{regs}) and *in vitro* T_{regs}. (**a**) T_{cons}, T_{regs}, and *in vitro* T_{regs} derived and pooled from spleen/lymph nodes (SPLN/LN) were stimulated for 4 days with α-CD3, α-CD28, and IL-2, and restimulated in the presence of TGF-β1 for 30 min. Flow cytometric contour plots show Foxp3 and pSmad2 (top) or pSMAD3 (bottom) staining of T_{con} (left), T_{reg} (middle), or iT_{reg} (right) cells. (**b**) % Apoptosis of T_{cons}, T_{regs}, or *in vitro* T_{regs} from wild-type (WT) or *Cd4-tgfβr2dn*^{tg} mice were restimulated as in Figure 2b without (white bars) or with 1 µg ml^{-1} (black bars) of α-CD3 antibody for 23 h. Data represent one of three independent experiments showing similar results. *P*-value is determined by Mann–Whitney test.

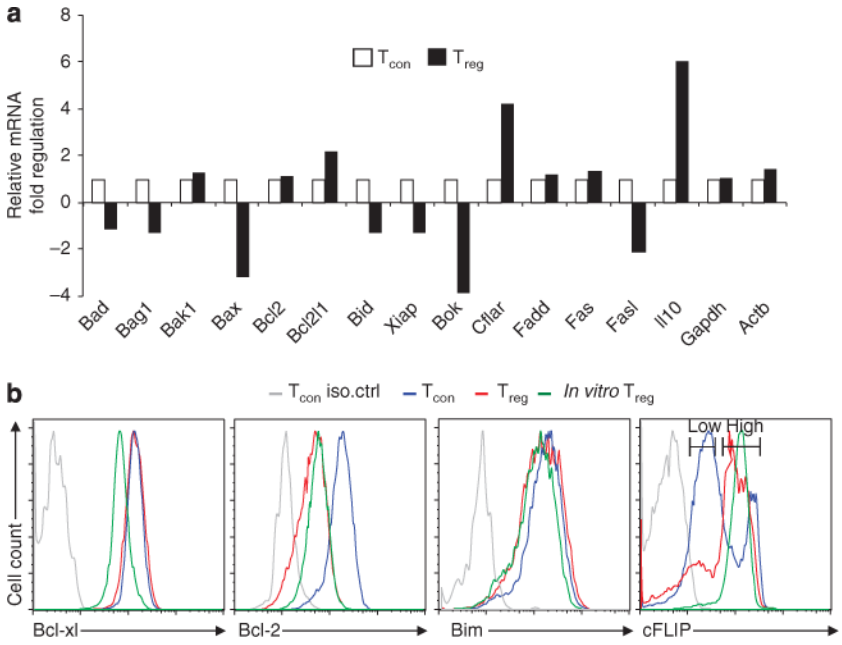

Figure 7.

Expression of apoptosis-related genes and proteins in regulatory T cells (T_{regs}). (**a**) T_{cons} and T_{regs} derived and pooled from spleen/lymph nodes (SPLN/LN) were restimulated as in Figure 2b. Total RNA was prepared 3 h after stimulation to assess the mRNA levels by quantitative PCR (qPCR) array using RT^2 Profiler PCR array (indicated by y axes). These data represent one of three independent experiments. (**b**) Flow cytometric histograms of T_{cons} (blue), T_{regs} (red), and *in vitro* T_{regs} (green) that were stimulated as above for 12 h, fixed, and stained for intracellular Bcl-xl, Bcl-2, Bim, and cFLIP (cellular FLICE (FADD-like IL-1β-converting enzyme)-inhibitory protein).

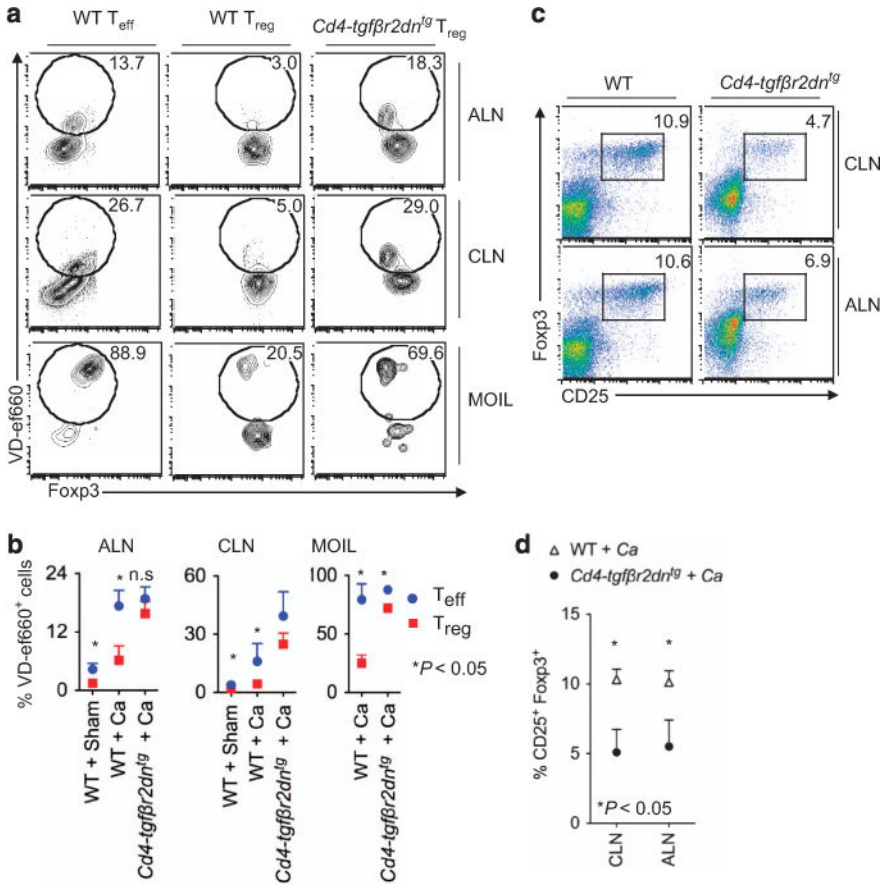

Figure 8.

Increased viability in regulatory T cells (T_{regs}) during *Candida* reinfection is transforming growth factor-β1 (TGF-β1) dependent *in vivo*. (**a**) *Rag1*$^{-/-}$ mice ($n = 11$) were reconstituted with CD4$^+$ cells from C57BL/6 or *Cd4-tgfβr2dn*^{tg} congenic mice. Recipient mice in each group were infected and reinfected with phosphate-buffered saline (PBS) sham controls or *Candida*. Axillary lymph nodes (ALNs), cervical lymph nodes (CLNs), and mouse oral intraepithelial and lamina propria leukocytes (MOIL) were harvested on day 1 after reinfection for examining cell death of Foxp3$^-$ T_{eff} in wild-type (WT) cell recipients (left), Foxp3$^{GFP+}T_{regs}$ in WT cell recipients (middle), and Foxp3$^{GFP+}T_{regs}$ in *Cd4-tgfβr2dn*^{tg} cell recipients (right) *ex vivo* by intracellular Foxp3 and VD-ef660 staining (gated on CD4$^+$ cells). (**b**) Quantification of the frequency of VD-ef660$^+$ dead cells among Foxp3$^-$ T_{effs} (blue circles) and Foxp3$^+$ T_{regs} (red squares) from ALNs, CLNs, MOIL, and inguinal lymph nodes (ILNs) as in **a** (gated on CD4$^+$ cells). Flow cytometric dot plots (**c**) and quantification (**d**) showing CD25- and Foxp3-expressing cells (T_{regs}) in WT cell recipients (**c**, left) and *Cd4-tgfβr2dn*^{tg} cell recipients (**c**, right) *ex vivo* (gated on CD4$^+$ cells) 2 days after reinfection as in **a**. Data represent three independent experiments showing similar results. Statistical significance was determined using Mann–Whitney test.